Wet Chemical Synthesis of CuO-PVA Hybrid Nanofluid Stabilized by Steric Repulsion

ANNIE AUREEN ALBERT[1,*,iD], D.G. HARRIS SAMUEL[2,iD] and V. PARTHASARATHY[1,iD]

[1]Department of Physics, Hindustan Institute of Technology and Science, Padur, Chennai-603103, India
[2]Department of Mechanical Engineering, Hindustan Institute of Technology and Science, Padur, Chennai-603103, India

*Corresponding author: E-mail: annieaahits@gmail.com

CuO-PVA hybrid nanofluid was synthesized within PVA matrix by a simple wet chemical precipitation method. The influence of rate of addition of precursor (NaOH) on the structure, morphology and stability of CuO-PVA hybrid nanofluids were studied. The structure was confirmed by XRD and UV-visible spectroscopy. High resolution transmission microscopy (HRTEM) images revealed the formation of smaller particles for addition of precursor in solid form or rapid addition (RA), whereas slow addition of precursor (SA) resulted in uniform particle size. The selected area electron diffraction (SAED) pattern of sample SA shows rings with small bright spots indicating that the sample is nano crystalline. The SAED pattern of sample RA shows diffuse rings with lesser number of bright spots indicating that it is less crystalline. The stability studies indicate that both the samples were stable for more than one year.

Keywords: Hybrid nanofluid, CuO nanoparticles, PVA, Dispersion, TEM, Zeta potential, Nanofluid stability.

INTRODUCTION

Nanofluids are a category of fluids in which nanoparticles are suspended in base fluids at low volume concentrations. Nanoparticles such as metals and metal oxides have been suspended in various basefluids with a motive of enhancing their thermophysical properties. Nanofluids are used in enhancing heat transfer [1-5], improving the efficiency of harvesting and storing energy [6-8], oil recovery [9], rheology [10] and drug delivery [11].

The principal problem encountered with these nanofluids is lack of stability, which affects the thermo-physical properties of the nanofluids. This is because the nanoparticles in the base fluid undergo Brownian motion and collide with one another. The van der Waals attractive force acting between the constituent particles during collision results in welding of the particles with each other leading to agglomeration and sedimentation of the nanoparticles. Thus the nanofluids lose their stability.

Different methods are applied to improve the stability of nanofluids [12], like reducing the particle size, dispersing the solid phase uniformly in the base fluids by methods like sonication, use of surfactants and by maintaining the pH well away from the isoelectric point. Often one or more methods are employed to achieve stability in nanofluids.

The use of surfactants is the easiest, most economical and widely used technique [13]. Surfactants prevent agglomeration of the nanoparticles by providing a repulsive force larger in magnitude compared to the van der Waals force acting between the particles. The repulsion may be electrostatic or steric repulsion. However, electrostatic stabilization has several drawbacks for example, nanofluids are stabilized kinetically, hence the particles cannot be redispersed once they aggregate and it can be used only for dilute nanofluids.

Steric stabilization employs a polymer molecule which is attached to the surface of nanoparticles by either physical adsorption or chemical bonding. The polymer chains provide an obstacle for the nanoparticles to come close to one another and screen the attractive forces. The solvent should be able to elongate the polymer chain to provide a good steric hindrance and prevent the particle from adhering to one another. Poly-(vinyl alcohol) (PVA) is a biocompatible polymer which degrades easily. It is hydrophilic and therefore the length of its molecular chain increases in water which enhances the steric repulsion nature of the polymer.

Stability of nanofluids is also highly influenced by the method of synthesis. Nanofluids can be synthesized either by single step or two step methods. In a single step method, the

nanoparticles are synthesized within the nanofluid and exhibit improved stability. Some of the few single step methods, *viz.* vacuum evaporation on running oil substrate (VEROS) [14,15], submerged arc nanoparticle synthesis system (SANSS) [16], pulsed wire evaporation (PWE) [17], pulsed laser ablation in liquids (PLAL) [18,19] and wet chemical method method [20] are generally are employed to synthesize the nanofluid.

Metal oxide nanoparticles are employed extensively as the solid phase dispersant in nanofluid because they offer several advantages. They are relatively less dense, easy to synthesize and chemically stable compared to the corresponding metal nanoparticles. The CuO nanofluid prepared with waste palm oil as base fluid showed a maximum stability of 6 months [4]. Zhu *et al*. [20] developed wet chemical method to synthesize stable CuO nanofluid which was stable for 5 months. They studied the influences of changing the metal precursor, its concentration and reaction time. The influence on rate of addition of the precursor has not been studied. Albert *et al*. [21] prepared CuO-PVA hybrid nanofluid which was stable up to 1 year and studied the thermal conductivity of the nanofluid at various temperatures and concentrations of nanofluid.

In this work, a single step wet chemical synthesis of CuO nanofluid with an eco-friendly surface modifier namely poly-(vinyl alcohol) (PVA) is reported. Here the advantages of steric repulsion offered by PVA and the enegy efficient simple wet chemical method have been used synergistically. This synthesis method does not involve the processes of centrifugation and calcination which are conducive for the growth of the particle leading to increase in size of the particle. The influence of rate of addition of precursor on the morphology and stability of the nanofluid has been analyzed.

EXPERIMENTAL

All the analytical grade chemicals *viz.* cupric nitrate trihydrate, poly(vinyl alcohol) of molecular weight 1,25,000, sodium hydroxide, *etc*. were procured from S.D. Fine-Chem. Ltd., Mumbai, India.

Characterizations: FTIR analysis was done with Thermo Nicolet Avatar 370 in the spectral range of 4000-400 cm^{-1}, using KBr beam splitter. The XRD analysis was done with Bruker AXSD8 Advance using Cu source (1.504 Å) for 2θ between10° to 100°. A Jeol/JEM 2100 HRTEM of 0.23nm point resolution was used for recording the images. The particle size estimation and zeta potential measurements were performed by dynamic light scattering using Malvern nanozeta sizer. Nanofluids were diluted suitably and the absorption spectra were recorded between 200 nm to 800 nm using JASCO UV Vis NIR Model V-670.

Preparation of CuO-PVA hybrid nanofluid: Poly(vinyl alcohol) (1 g) was dissolved in 100 mL of deionized water at 60 °C under constant stirring and then 0.1 M of Cu(NO$_3$)$_2$·3H$_2$O was added to this solution under continuous stirring for 30 min. Sodium hydroxide pellets (6 g) were added to PVA-Cu(II) solution and reaction was continued for 1 h. The solution was kept aside without disturbing for 1 h. Black gel like precipitate settled at the bottom in large quantities. The sediment was recovered by decanting the clear supernatant. The recovered precipitate was washed with deionized water several times.

The sediment was then transferred to 200 mL of deionized water and sonicated for 105 min. This sample was designated as rapid addition (RA).

Similarly, the aforesaid procedure was carried out with 6 g of NaOH dissolved in 100 mL of deionized water by adding it dropwise at a slow rate. This sample was designated as slow addition (SA). The CuO-PVA gel was prepared by the above method once again and dried in hot air oven at 60 °C.

RESULTS AND DISCUSSION

FTIR analysis: The FTIR spectrum of hybrid nanofluids is shown in Fig. 1. The broad peak between 3500-3000 cm^{-1} is characteristic of OH group which is present in PVA [22] and water [23]. The broad band at 2079 cm^{-1} can be attributed to carbonyl group in the acetate residue present in PVA. The absorption peak at 1637 cm^{-1} arises due to C=C group because of inter/intra molecular bond formed by hydrogen of PVA and neighboring OH groups [24]. Peaks at 575 and 538 cm^{-1} can be attributed to the formation of CuO.
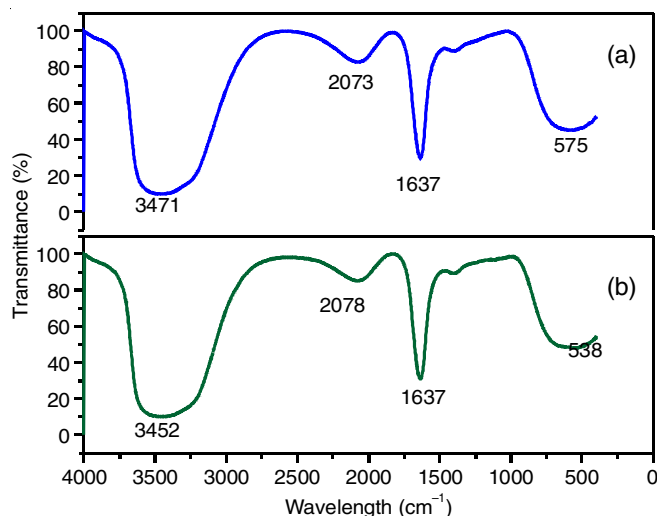

Fig. 1.   FTIR of CuO-PVA hybrid nanofluid prepared by (a) slow addition of precursor (SA) and (b) rapid addition of precursor (RA)

XRD analysis: The diffraction peaks for the dried sample are shown in Fig. 2. The peak values in the pattern matched with the ICDD data for CuO file no 80-1916 [22] confirming the formation of monoclinic CuO. The first two low intensity peaks at 19.4° and 23.5° were due to PVA, which has the semi-crystalline nature [23].

UV-visible analysis: The nanofluid was studied for one month visually for sedimentation. The CuO-PVA hybrid nanofluids samples SA and RA showed no marked sedimentation. The UV spectra for the samples *i.e.*, by process of slow addition and rapid addition (Fig. 3) show broad absorption band at 283 nm. This is due to the formation of nano CuO [25]. The decrease in absorption spectra in the region 300-400 nm is characteristic of PVA [26]. The absorbance of nanofluid is directly proportional to the concentration of particles dispersed in the nanofluid. This gives an indication of stability of the nanofluid. From Fig. 3, it is also evident that both the samples showed same level of absorbance, which indicates that both hybrid nanofluid samples exhibited equally good stability.
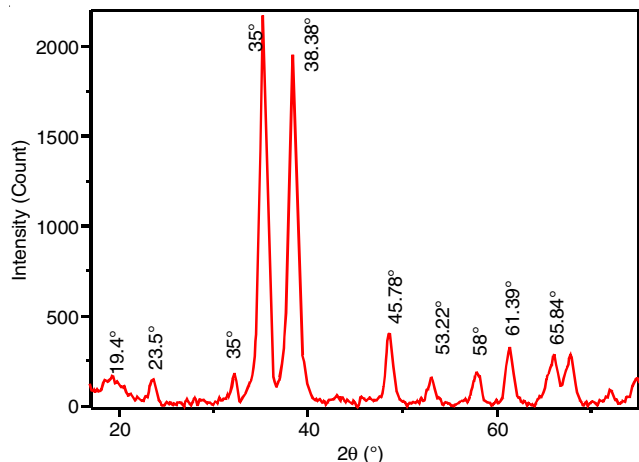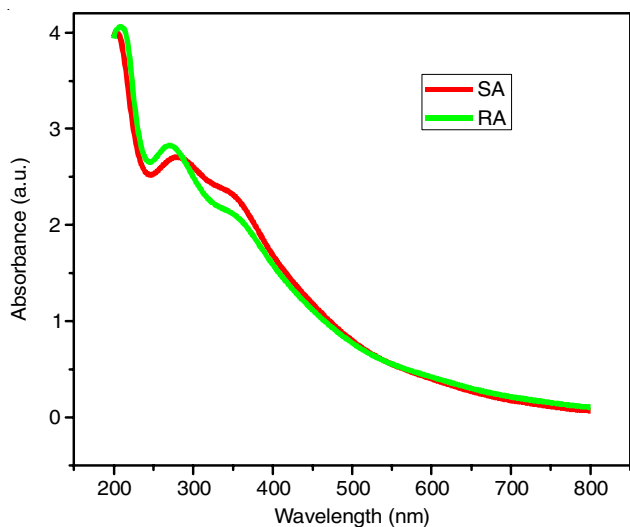
Fig. 2. XRD pattern of CuO-PVA nanocomposite

Fig 3. UV absorption spectra of CuO-PVA hybrid nanofluid prepared by (a) slow addition of precursor (SA) and (b) rapid addition of precursor (RA)
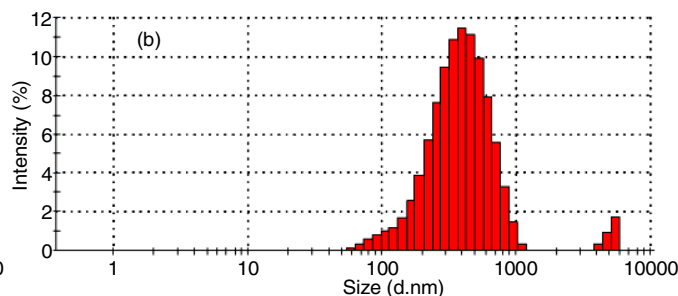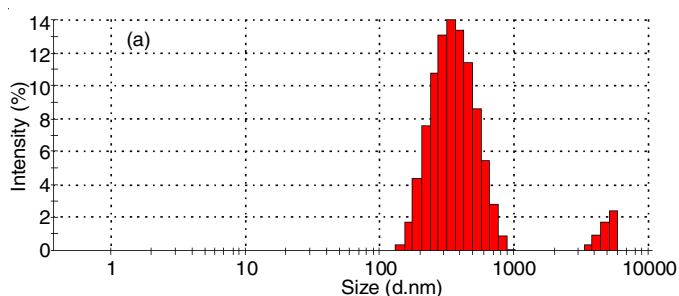
Particle size: The size of nanoparticles in CuO-PVA hybrid nanofluids was determined by dynamic light scattering method. The results for the samples prepared by slow addition and rapid addition of NaOH are shown in Fig. 4. The determined particle size values in both cases of CuO-PVA nanofluids were found to be nearly similar.

Zeta potential: Zeta potential measurement gives an estimate of stability of nanofluid. It measures the difference in potential between the stern layer of dispersed phase (nanoparticles) and the dispersion medium (base fluid). Absolute values of zeta potential greater than 30 mV was observed for electrostatical stabilized nanofluids. Zeta potential values of -10 and -12 mV for the samples SA and RA were lower than expected as shown in Fig. 5a & 5b, respectively. This is because the stability imparted to the hybrid nanofluid arised out of the steric hindrance effect provided by PVA molecules.

Photo capturing: Photo capturing is another tool to study the stability of nanofluids. Fig. 6 shows the photograph of the samples SA and RA taken after one year of synthesis of the hybrid nanofluids. It can be seen that there is no separation of base fluid and the solid dispersant. There is no trace of sedimentation, which indicated that the synthesized samples SA and RA are equally stable.

HRTEM analysis: The micrographs of PVA-CuO hybrid nanofluids prepared by slow addition (SA) and rapid addition (RA) of NaOH are shown in Fig. 7. It can be observed that both the images showed spherical CuO crystallites embedded in the PVA matrix. The nanoparticles were slightly bigger and uniform in size with better dispersion for dropwise addition (SA) of NaOH pellets whereas it was smaller but non-uniformly dispersed for addition of NaOH pellets (RA).

SAED analysis: Fig. 8 shows the SAED patterns for PVA-CuO hybrid nanofluids prepared by dropwise solution and NaOH pellets. In Fig. 8a, the rings are clear with more number of small bright spots indicating the crystalline nature

Fig. 4. Particle size analysis of CuO-PVA hybrid nanofluid prepared by (a) drop-wise addition of precursor and (b) rapid addition of precursor
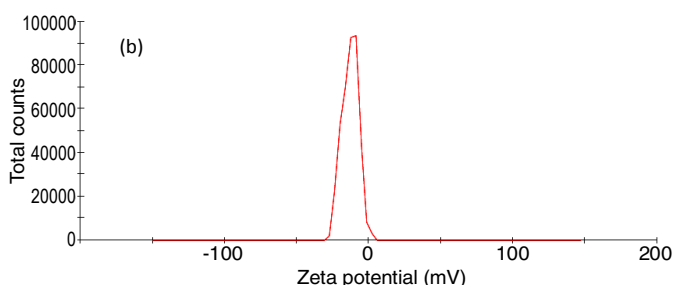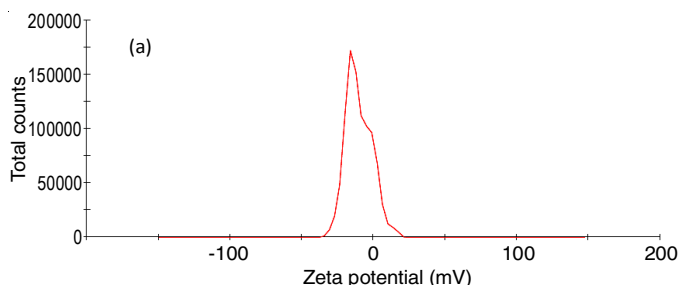

Fig. 5. Zeta potential measurement of CuO-PVA hybrid nanofluid prepared by (a) drop wise addition of precursor and (b) rapid addition of precursor
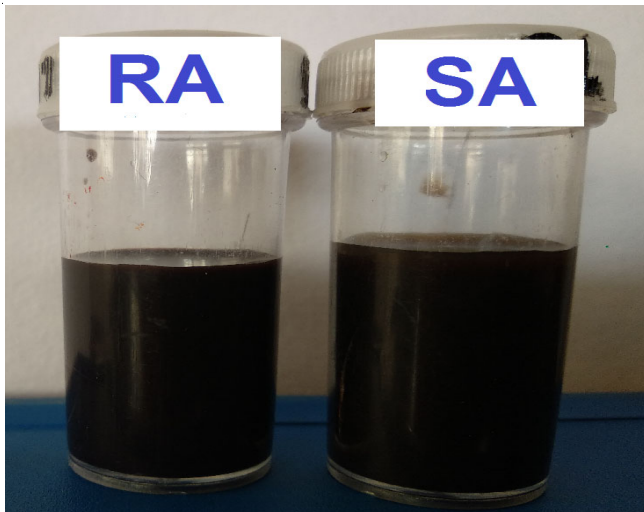
Fig. 6.   Photograph of CuO-PVA hybrid nanofluid after one year of synthesis prepared by (a) rapid addition (RA) of precursor in solid form and (b) SA addition or slow addition (SA) of precursor

of CuO nanoparticles embedded in the PVA matrix for dropwise addition of NaOH solution. The same type of composite is less crystalline in nature due to addition of NaOH as pellets. This can be inferred from the diffuse nature of the rings in Fig. 8b, which has few scattered bright spots.

Conclusion

The structural conformation for CuO-PVA nanofluids was done by XRD analysis. It revealed the formation of monoclinic CuO. The UV absorption spectra shows that the rate of addition of the precursor had no marked influence on the stability of nanofluid. The particle size analysis of the samples showed that both samples SA and RA of NaOH pellets were almost same in size. Zeta potential analysis confirmed the steric stabilization of CuO-PVA hybrid nanofluids. HRTEM micrographs showed that the CuO nanoparticles are more uniformly distributed and slightly larger in size for the sample SA when compared to sample RA. The SAED characterization shows the particles to be more crystalline for SA sample in comparison
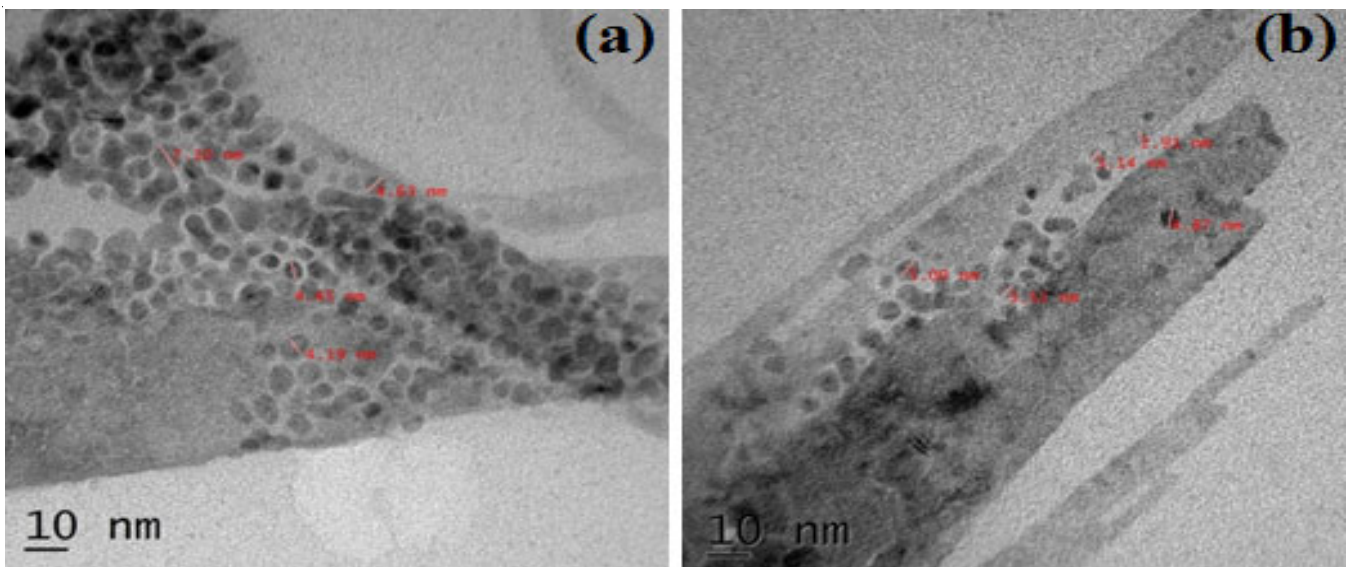

Fig. 7. HRTEM images of CuO-PVA hybrid nanofluid prepared by (a) drop wise addition of precursor and (b) rapid addition of precursor
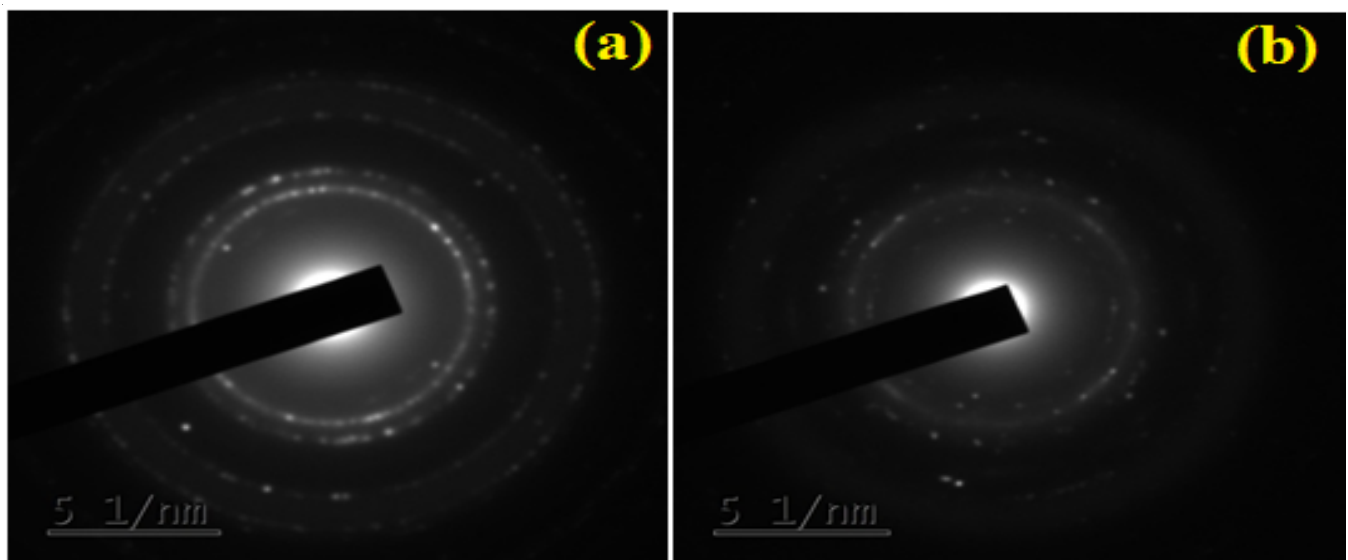

Fig. 8. SAED patterns of CuO-PVA hybrid nanofluid prepared by (a) drop wise addition of precursor and (b) rapid addition of precursor

with RA sample. It can be concluded that the sample prepared by dropwise addition of NaOH (SA sample) resulted in better crystalline nature than the sample prepared by addition of NaOH pellets (RA sample) and both the samples were stable upto 1 year. The enhanced stability is due to the synergistic effect of single step synthesis and the steric stabilization techniques.

CONFLICT OF INTEREST

The authors declare that there is no conflict of interests regarding the publication of this article.

REFERENCES

1. S. Yan, H. Zhang, F. Wang, R. Ma, Y. Wu and R. Tian, *J. Renew. Sustain. Energy*, **10**, 063704 (2018);
    https://doi.org/10.1063/1.5051207
2. T.S. Krishnakumar, A. Sheeba, V. Mahesh and M.J.Prakash, *Int. J. Refrig.*, **102**, 55 (2019);
    https://doi.org/10.1016/j.ijrefrig.2019.02.035
3. V. Mikkola, S. Puupponen, K. Saari, T. Ala-Nissila and A. Seppälä, *Int. J. Therm. Sci.*, **117**, 163 (2017);
    https://doi.org/10.1016/j.ijthermalsci.2017.03.024
4. M. Javed, A.H. Shaik, T.A. Khan, M. Imran, A. Aziz, A.R. Ansari and M.R. Chandan, *Heat Mass Transfer*, **54**, 3739 (2018);
    https://doi.org/10.1007/s00231-018-2399-y
5. S.K. Soylu, I. Atmaca, M. Asiltürk and A. Dogan, *Appl. Therm. Eng.*, **157**, 113743 (2019);
    https://doi.org/10.1016/j.applthermaleng.2019.113743
6. N. Navarrete, R. Mondragón, D. Wen, M.E. Navarro, Y. Ding and J.E. Juliá, *Energy*, **167**, 912 (2019);
    https://doi.org/10.1016/j.energy.2018.11.037
7. S. Harikrishnan, A. Devaraju, G.R. Kumar and S. Kalaiselvam, *Mater. Today Proc.*, **9**, 410 (2019);
    https://doi.org/10.1016/j.matpr.2019.02.170
8. J.G. Monroea, S. Kumari, J.D. Fairley, K.B. Walters, M.J. Berge and S.M. Thompsonf, *Int. J. Heat Mass Transfer*, **132**, 162 (2019);
    https://doi.org/10.1016/j.ijheatmasstransfer.2018.11.096
9. M.I. Youssif, R.M. El-Maghraby, S.M. Saleh and A. Elgibaly, *Egypt. J. Pet.*, **27**, 105 (2018);
    https://doi.org/10.1016/j.ejpe.2017.01.006
10. L. Kong, J. Sun and Y. Bao, *RSC Adv.*, **7**, 12599 (2017);
    https://doi.org/10.1039/C6RA28243A
11. L. Zhang, J. Xia, Q. Zhao, L. Liu and Z. Zhang, *Small*, **6**, 537 (2010);
    https://doi.org/10.1002/smll.200901680
12. F. Yu, Y. Chen, X. Liang, J. Xu, C. Lee, Q. Liang, P. Tao and T. Deng, *Prog. Nat. Sci. Mater. Int.*, **27**, 531 (2017);
    https://doi.org/10.1016/j.pnsc.2017.08.010
13. D. Dey, P. Kumar and S. Samantaray, *Heat Transfer*, **46**, 1413 (2017);
    https://doi.org/10.1002/htj.21282
14. S. Yatsuya, Y. Tsukasaki, K. Mihama and R. Uyeda, *J. Cryst. Growth*, **45**, 490 (1978);
    https://doi.org/10.1016/0022-0248(78)90481-5
15. H. Akoh, Y. Tsukasaki, S. Yatsuya and A. Tasaki, *J. Cryst. Growth*, **45**, 495 (1978);
    https://doi.org/10.1016/0022-0248(78)90482-7
16. C.H. Lo, T.T. Tsung and L.C. Chen, *J. Cryst. Growth*, **277**, 636 (2005);
    https://doi.org/10.1016/j.jcrysgro.2005.01.067
17. G.J. Lee, C.K. Kim, M.K. Lee, C.K. Rhee, S. Kim and C. Kim, *Thermochim. Acta*, **542**, 24 (2012);
    https://doi.org/10.1016/j.tca.2012.01.010
18. T.X. Phuoc, Y. Soong and M.K. Chyu, *Opt. Lasers Eng.*, **45**, 1099 (2007);
    https://doi.org/10.1016/j.optlaseng.2007.06.005
19. S.W. Lee, S.D. Park and I.C. Bang, *Int. J. Heat Mass Transf.*, **55**, 6908 (2012);
    https://doi.org/10.1016/j.ijheatmasstransfer.2012.07.004
20. H. Zhu, D. Han, Z. Meng, D. Wu and C. Zhang, *Nanoscale Res. Lett.*, **6**, 181 (2011);
    https://doi.org/10.1186/1556-276X-6-181
21. A.A. Albert, D.G.H. Samuel, V. Parthasarathy and K. Kiruthika, *Chem. Eng. Commun.*, **207**, 319 (2020);
    https://doi.org/10.1080/00986445.2019.1588731
22. P. Yugandhar, T. Vasavi, Y. Jayavardhana Rao, P. Uma Maheswari Devi, G. Narasimha and N. Savithramma, *J. Cluster Sci.*, **29**, 743 (2018);
    https://doi.org/10.1007/s10876-018-1395-1
23. C.M. Tang, Y.H. Tian and S.H. Hsu, *Materials*, **8**, 4895 (2015);
    https://doi.org/10.3390/ma8084895
24. S. Gandhi, R.H.H. Subramani, T. Ramakrishnan, A. Sivabalan, V. Dhanalakshmi, M.G. Nair and R. Anbarasan, *J. Mater. Sci.*, **45**, 1688 (2010);
    https://doi.org/10.1007/s10853-009-4158-4
25. S. Felix, R.B.P. Chakkravarthy and A.N. Grace, *IOP Conf. Series Mater. Sci. Eng.*, **73**, 012115 (2015);
    https://doi.org/10.1088/1757-899X/73/1/012115
26. O.G. Abdullah, B.S. Aziz, K.M. Omer and Y.M. Salih, *J. Mater. Sci. Mater. Electron.*, **26**, 5303 (2015);
    https://doi.org/10.1007/s10854-015-3067-3